J1.5

IMPROVEMENT OF THE PRECIPITATION PROCESSES IN THE JMA HIGH-RESOLUTION GLOBAL NWP MODEL AND ITS IMPACT STUDY FOR TROPICAL CYCLONE CASES

Takuya Komori *
Japan Meteorological Agency, Tokyo, JAPAN

1. INTRODUCTION

The Japan Meteorological Agency (JMA) has a plan for a current operational Global Spectral Model (GSM) to enhance the horizontal resolution (from 60 km to 20 km) and the vertical resolution (from 40 layers to 60 layers) in November 2007, with the aim of improving the model's ability to forecast high impact weather such as tropical cyclones (TCs).

Associated with the resolution enhancement and the implementation of the new GSM [with a horizontal resolution of 20km and a vertical resolution of 60 layers (TL959L60, hereafter called "20km GSM")], the Regional Spectral Model (RSM) [with a horizontal resolution of 20km] and the Typhoon Model (TYM) [with a horizontal resolution of 24km] will be replaced by the 20km GSM.

Outlined below are the overviews of TC forecast performance and impact studies to improve the precipitation processes in the 20km GSM.

2. OUTLINE OF THE 20km GSM IN JMA

JMA upgraded the supercomputer system in March 2006, which is a distributed-memory parallel computer, Hitachi SR11000 (80 nodes x2), with a peak performance of 21.5 Tflops and main memory of 10.0 Tbytes (previous supercomputer was Hitachi SR8000 with a peak performance of 768 Gflops and main memory of 640 Gbytes). The current system is the eighth generation since an IBM 704 was first installed in 1959 (JMA 2007).

Figure 1 shows model topography around Japan of the 20km GSM and the 60km GSM (TL319L40: the current GSM with the horizontal resolution of 60km and the vertical resolution of 40 layers). Since the 20km GSM can resolve the topography more efficiently than the 60km GSM, better performance with orographic precipitation can be expected in the 20km GSM.

Figure 2 shows the vertical level distribution of the 20km GSM (blue line) and the 60km GSM (red line), respectively. It is found that the enhancement of vertical resolution is notable in the upper level (from 10hPa to 100hPa) and the lower level (from 600hPa to 900hPa). In this regard, one may also notice that the 20km GSM has a top level of 0.1hPa, while the 60km GSM has a top level of 0.4hPa.

Figure 3 shows anomaly correlation scores of sea level pressure averaged for global area in August and September 2004. There can be seen a slight improvement in the 20km GSM, although the 20km GSM has almost the same performance as the 60km GSM.

3. FORECAST PERFORMANCE OF TROPICAL CYCLONE

Due to tremendous efforts, the accuracy of the JMA operational forecasts with GSM has been improving step by step over the last 15 years, although interannual variability is found in the accuracy of tropical cyclone (TC) forecast (Komori et al. 2007).

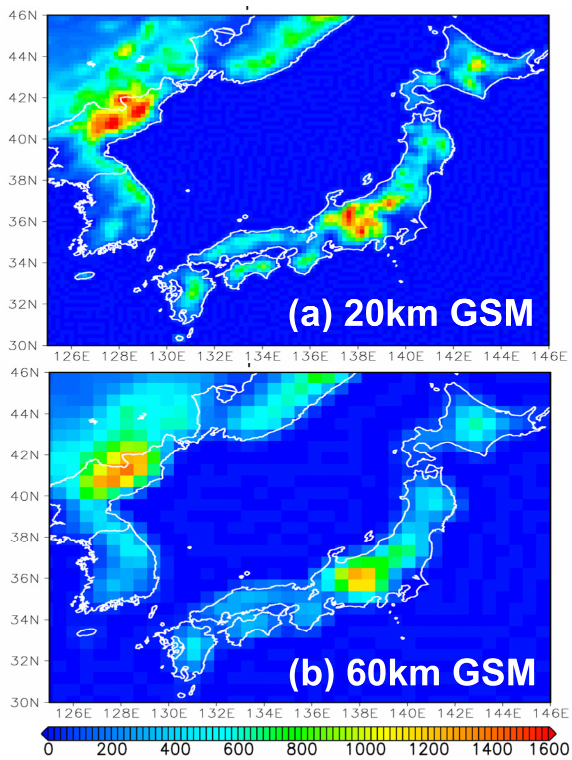

Figure 1: Model topography around Japan of (a) 20km GSM (TL959L60) and (b) 60km GSM (TL319L40).

* *Corresponding author address:* Takuya Komori, Numerical Prediction Division, Japan Meteorological Agency, 1-3-4 Otemachi, Chiyoda-ku, Tokyo 100-8122, Japan; e-mail: komori@met.kishou.go.jp

For typhoon forecasts over the western North Pacific, bogus typhoon data are assimilated to supplement the TC structure in the initial field of forecast models. The 20km GSM uses the new bogus typhoon profiles which serve as observation pseudo-data in the global cycle analysis. In the current global cycle analysis, the bogus data structure is implanted into the first guess fields by a blending method with a linear weighting function.

Figure 5 shows TC forecast position errors (line graph) and the number of samples used in the verification (bar graph) by Murakami et al. (2007). Forecasts by the 20km GSM and the 60km GSM are shown with a blue line and a red line, respectively. This figure represents the performance of the TC track forecast of the 20km GSM is almost the same as that of the 60km GSM.

Figure 6 shows the case study for 90-hour TC forecasts for the typhoon Songda in the western North Pacific Ocean at all initial times from 00 UTC 28 August 2004 to 00 UTC 08 September 2004. The solid black line indicates the analysed TC track. The TC track forecasts of the 20km GSM (blue lines) are similar to those of the 60km GSM (red lines).

The forecast performance of central pressure and maximum sustained wind speed for typhoon Songda demonstrates that the 20km GSM provides better forecasts of these elements than the 60km GSM (Figure 7).

From these verification results, the enhancement of horizontal and vertical resolution seems to be much more effective for TC intensity forecast. For a TC track forecast, it may be more important to resolve large-scale environmental contexts surrounding the TCs than to resolve the inner structure.

4. IMPACT STUDIES TO IMPROVE THE PRECIPITATION PROCESSES IN THE 20km GSM

The physical processes of the 20km GSM are basically the same as those of the 60km GSM. The 60km GSM's convection scheme is the prognostic Arakawa-Schubert cumulus scheme with convective momentum transport. The 60km GSM also uses the prognostic cloud scheme similar to that of Smith (1990); the Marine storatocumulus scheme proposed by Kawai and Inoue (2006); and the boundary layer scheme of Mellor–Yamada level 2 closure.

Since the 20km GSM has the enhancement of the horizontal and the vertical resolution, the above physical processes of the GSM may change the precipitation balance between grid and subgrid scale precipitation processes, and we may have to adjust the precipitation processes to suit the 20km horizontal resolution.

One of the most important physical processes that play a crucial role in numerical weather prediction is the cumulus convection. Since the assumption that an ensemble of cumulus clouds is contained in a single column from the model in the Arakawa-Schubert cumulus parameterization scheme may induce resolution dependency, precipitation forecasts simulated by the 20km GSM and the 60km GSM are compared with observations (Nakagawa, 2005).

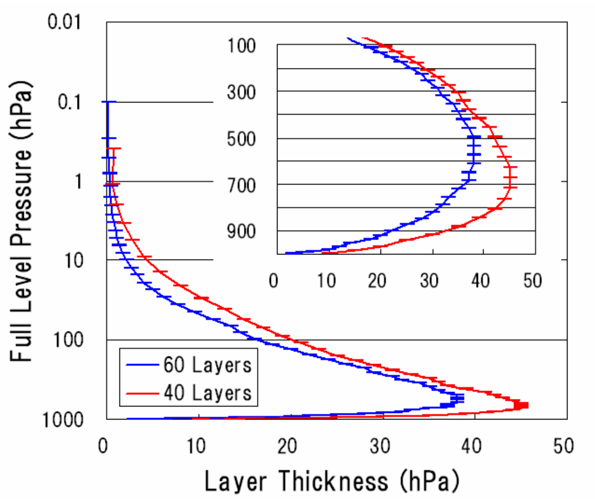

Figure 2: Vertical level distribution of the 20km GSM (TL959L60: blue line) and the 60km GSM (TL319L40: red line). The abscissa represents layer thickness (hPa), while the ordinate represents full level pressure (hPa).

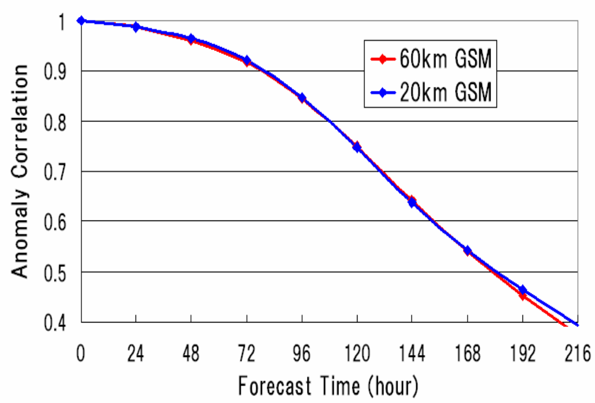

Figure 3: Anomaly correlation scores of sea level pressure for global area with the 20km GSM (blue line) and the 60km GSM (red line), which is averaged for August and September 2004.

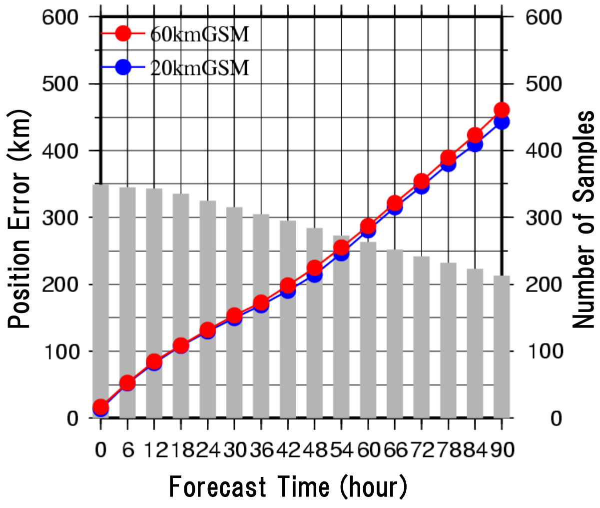

Figure 5: TC forecast position errors (line graph) and the number of samples used in the verification (bar graph) for the western North Pacific Ocean. Forecasts by the 20km GSM and the 60km GSM are shown in a blue line and a red line, respectively (Murakami et al. 2007).

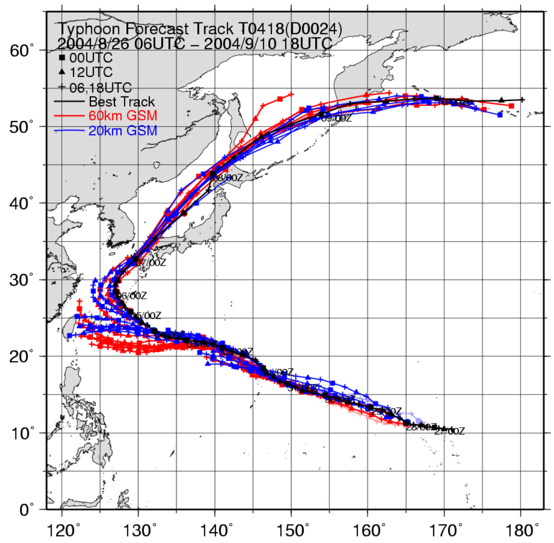

Figure 6: The case studies for the typhoon Songda in the western North Pacific Ocean at all initial times. The solid black line indicates the analysed TC track. Forecasts by the 20km GSM and the 60km GSM are shown in the blue lines and the red line, respectively.

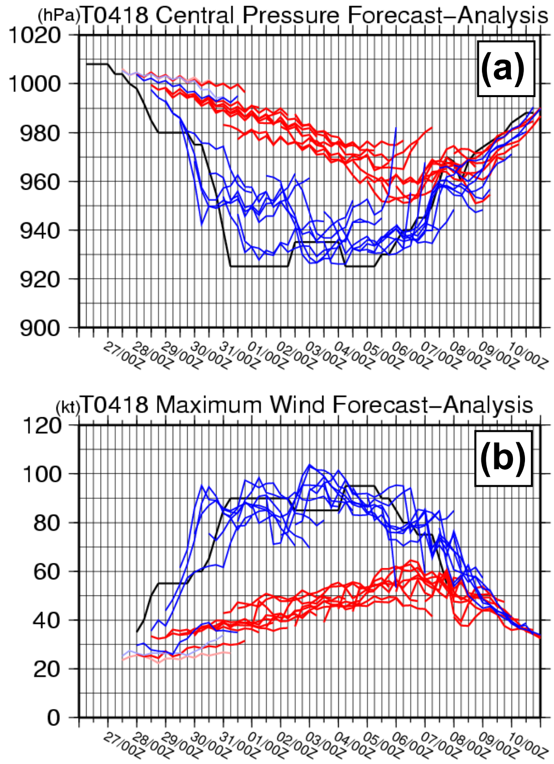

Figure 7: Forecasts with the 20km GSM (blue lines) and the 60km GSM (red lines) in (a) central pressure and (b) maximum sustained wind speed for the typhoon Songda in the western North Pacific Ocean. The solid black line indicates the analysed value.

Figure 8 shows the 6-hour accumulated rain by observation with radar and rain gauge (8a) and NWP models (8b, 8c and 8d) for 24-hour forecast at the initial time of 12 UTC 17 July 2005 in Japan area. Figure 8c demonstrates that the 20km GSM has better performance for orographic precipitation than the 60km GSM (Figure 8b), although the area of simulated weak precipitation is wider than the observation. Some investigations reveal that this weak precipitation is induced by subgrid scale precipitation processes in the case of convective unstable environment.

To address the issue of the wider area of simulated weak precipitation, the convection triggering mechanism proposed by Xie and Zhang (2000) was introduced in the 20km GSM.

Xie and Zhang (2000) showed a strong relationship between deep convection and the positive dynamic CAPE generation rate (DCAPE) determined by the large scale advective tendencies of both temperature and moisture. From the results of an investigation of DCAPE with the 20km GSM and the 60km GSM, Nakagawa (2005) indicated that the triggering function for deep convection can be used to improve the precipitation forecast. Figure 8d demonstrates the impact of the new convection triggering function in comparison with Figure 8c.

For the forecast performance of TCs, due to the resolution enhancement and the introduction of the convection triggering mechanism, better performance can be expected in the 20km GSM.

Figure 9 shows 12-hour accumulated rain (colored) and sea level pressure (contour) for the typhoon Chaba in the western North Pacific Ocean for 24-hour forecast at the initial time of 12 UTC 29 August 2004. The contour interval of sea level pressure is 4hPa.

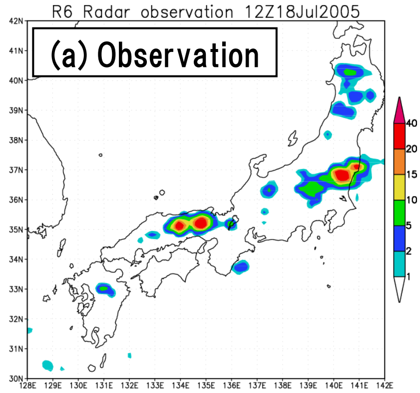

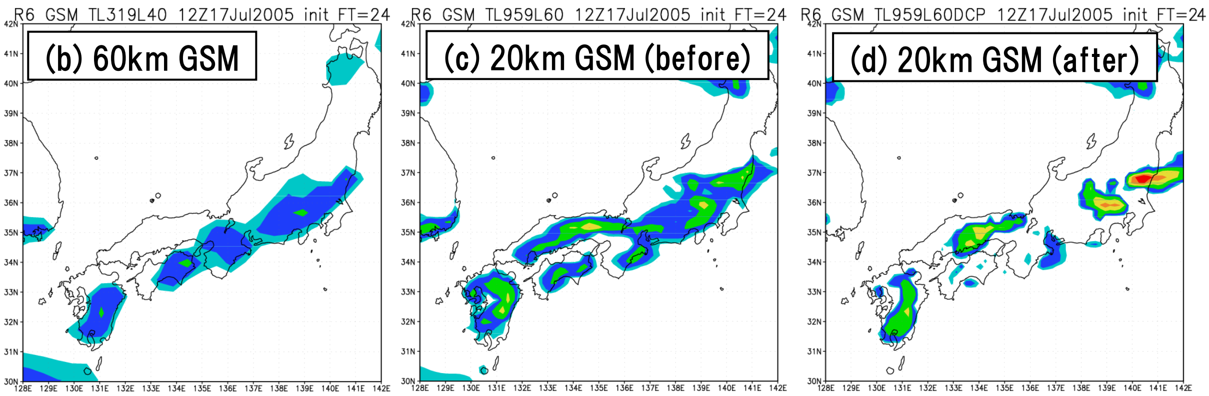

Figure 8: 6-hour accumulated rain (mm) of (a) observation (radar and rain gauge), (b) 60km GSM, (c) 20km GSM and (d) 20km GSM with new convection triggering function for 24-hour forecast at the initial time of 12 UTC 17 July 2005 (Nakagawa 2005).

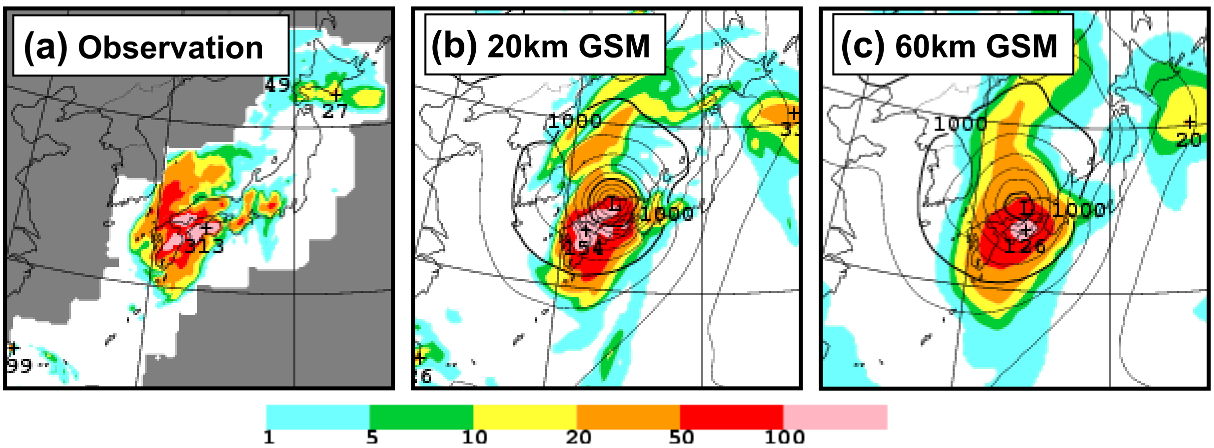

Figure 9: 12-hour accumulated rain (mm) (shaded) and sea level pressure (hPa) (contours) from (a) observation (radar and rain gauge) and 24-hour forecast of (b) 20km GSM with new convection triggering function and (c) 60km GSM for the typhoon Chaba in the western North Pacific Ocean at the initial time of 12 UTC 29 August 2004. The contour interval of sea level pressure is 4hPa.

From this figure, the 20km GSM seems to give more accurate of orographic precipitation than the 60km GSM, especially for the area range of precipitation for more than 100mm. The 20km GSM also has a deeper central pressure for the TC than the 60km GSM, which is the same impact as the case study for the typhoon Songda (Figure 7).

Since direct comparison with the satellite image is helpful to assess the performance of TC forecasts by NWP models, simulated satellite images are also verified. To simulate satellite image, the brightness temperature is calculated using a radiative transfer model based on the method of the GSM (Oowada 2006).

It is found that the 20km GSM with the new convection triggering function (Figure 10d) provides more distinct TC structure and better cloud simulations than the 60km GSM (Figure 10b) according to the results of the comparison with the GOES-9 satellite image (Figure 10a) at 00 UTC 29 August 2004 for the typhoon Chaba.

It is also found that the TC eye simulated by the 20km GSM is not as distinct as the observed eye in the GOES-9 satellite image. To address this issue, we reduce the intensity of convective momentum transport in Arakawa-Schubert cumulus scheme and also modify the probability density function of the total water representing deep cumulus clouds. These modifications change the precipitation balance resulting in greater amounts of subgrid scale precipitation and lesser amounts of grid scale precipitation. Consequently, these modifications of the precipitation processes in the 20km GSM provide a more distinct TC eye structure (Figure 10c).

The rain accumulated over 3 hours is also compared with radar observation data in Figure 11. Figures 11b, 11c and 11d are corresponding to the results in Figures 10b, 10c and 10d, respectively. The contour interval of sea level pressure is 5hPa. Compared with Figures 11c and 11d, the modifications of the precipitation processes seem to make a less amount of rain in the TC central area. This result shows the characteristics consistent with the results of the satellite image comparison in Figures 10c and 10d.

In the comparison with the GOES-9 satellite image (Figure 10a) and the radar observation data (Figure 11a), we further find the TC horizontal size simulated by the modified 20km GSM seems to be smaller, and the simulated clouds in some areas around the TC seem to not be dense enough. This feature is more clearly evident in the development stage of TCs.

Figure 12 shows the time evolution of surface wind speed simulated by (a) 60km GSM and (b) 20km GSM for the typhoon Songda in its development stage. The surface wind speed at each forecast time is shown in solid colored lines. The colored triangles represent the radii with 30kt and 50kt wind speed analyzed in operation at each valid time.

In this figure, the radii of the 30kt and 50kt wind speeds simulated by the 20km GSM at every forecast time are shorter than those of the analysis in operation. This result is consistent with the smaller TC structure in the 20km GSM showed in Figures 10 and 11, although the 60km GSM has weaker wind speed and a very gradual structure.

From the results above, it is found that the 20km GSM generally provides better forecasts than the 60km GSM, and however further investigations are needed to improve TC horizontal size and eye, especially in the TC development stage.

5. SUMMARY AND FUTURE PLANS

This paper overviewed TC forecast performance and our trials to improve the precipitation processes of the 20km GSM which will be the JMA operational Model in November 2007.

The resolution enhancement can be expected to improve the model's ability to forecast high impact weather such as TCs. As for the performance of the TC track forecast, statistical verification shows that the forecast position error by the 20km GSM is almost the same as that of the 60km GSM. On the other hand, the performance of the TC intensity forecast of the central pressure and the maximum sustained wind speed demonstrates that the 20km GSM provides better forecasts than the 60km GSM. These results suggest that addressing the problem of TC intensity forecasts would need the enhancement of the model resolution.

We also investigate the cloud and precipitation characteristics of the 20 km GSM in several case studies. Since the 20km GSM can resolve the topography more efficiently than the 60km GSM, the better expression of orographic precipitation can be shown in the 20km GSM.

The new triggering function for deep convection introduced by Nakagawa (2005) can be used to improve the precipitation forecast in the case of convective unstable environment.

In some investigations, we find that the modification of the precipitation processes provide a more distinct TC eye structure according to the results of the direct comparison between the GSM simulated images and the GOES-9 satellite image.

This result shows the characteristics consistent with the result of the comparison with the rain accumulated over 3 hours.

These comparisons additionally show that the TC horizontal size simulated by the 20km GSM seems to be small and simulated clouds in the area around the TC seem to not be dense enough. This is supported by the result of the comparison with the 20km GSM and operational analysis in radii of the 30kt and 50kt wind speeds, especially in the TC development stage. The further investigations are needed to improve TC horizontal size and eye.

For developing the global NWP model, since the accuracy of TC forecasts shows the performance of the global model in the tropics and subtropics, evaluation and address of the issues mentioned above for TC forecast can be very important. To more efficiently evaluate the performance of the 20km GSM, the usage of the observation data of cloud and atmosphere with high-resolution vertical and horizontal profiles is essential. Hence, the verification using new satellite observation data such as CloudSat and AIRS will possibly be important in follow-up research.

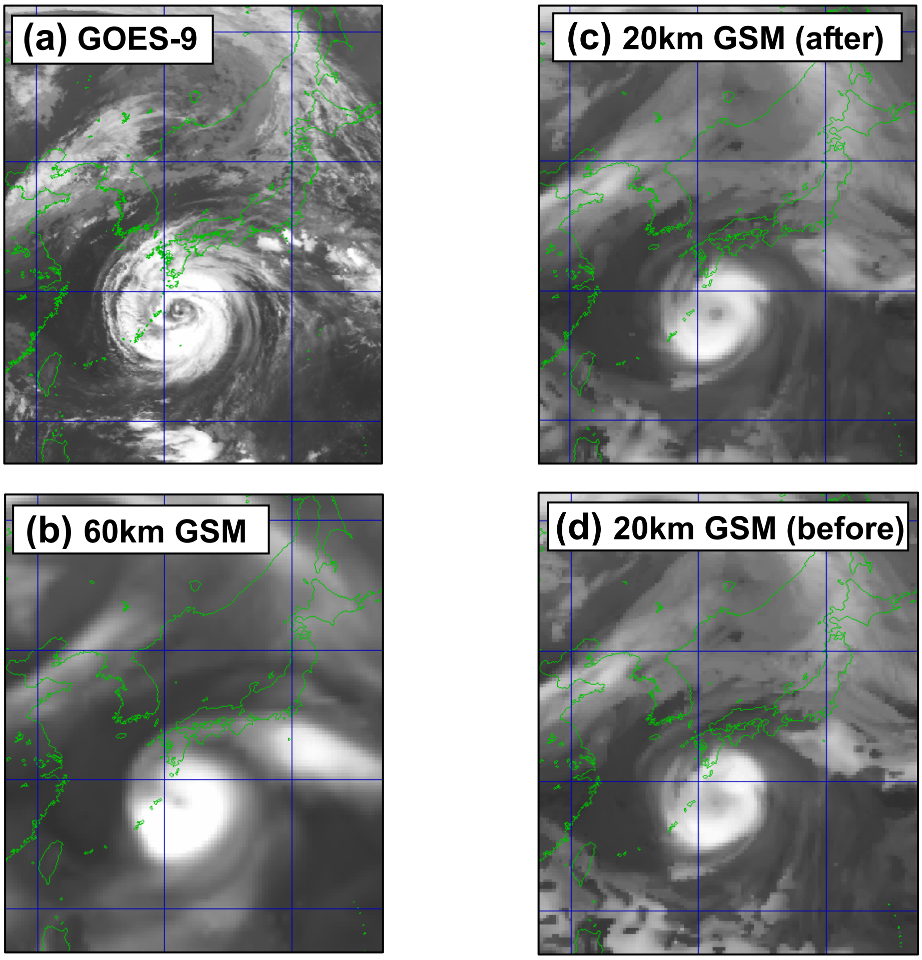

Figure 10: Observed and simulated infrared satellite Image at 00 UTC 29 August 2004 for the typhoon Chaba in the western North Pacific Ocean: (a) GOES-9, (b) 60km GSM, (c) 20km GSM with both the new convection triggering function and modifications of precipitation processes, (d) 20km GSM with the new convection triggering function.

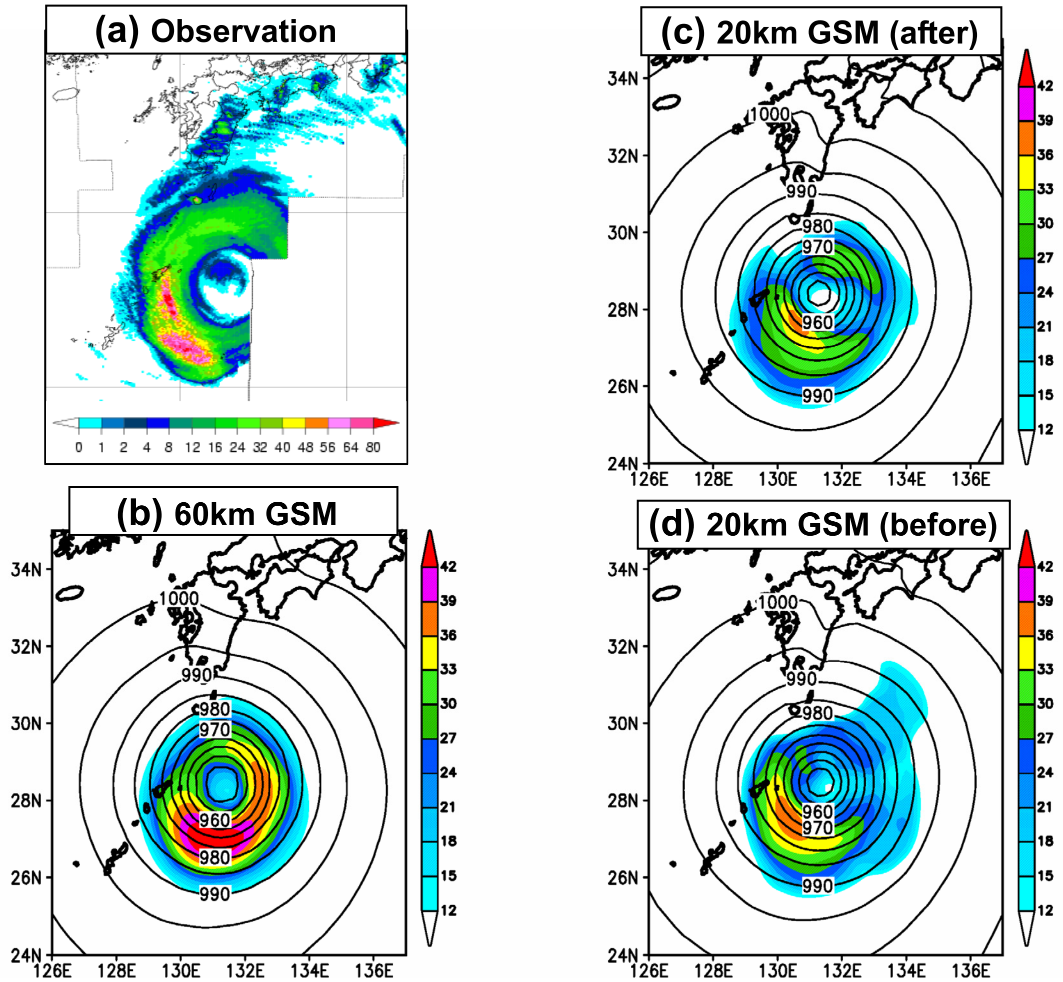

Figure 11: Observed and simulated rain accumulated over 3 hours (mm) (shaded) and sea level pressure (hPa) (contours): (a) observation (radar). (b), (c) and (d) are corresponding to Figure 10b, 10c and 10d, respectively. The contour interval of sea level pressure is 5hPa.

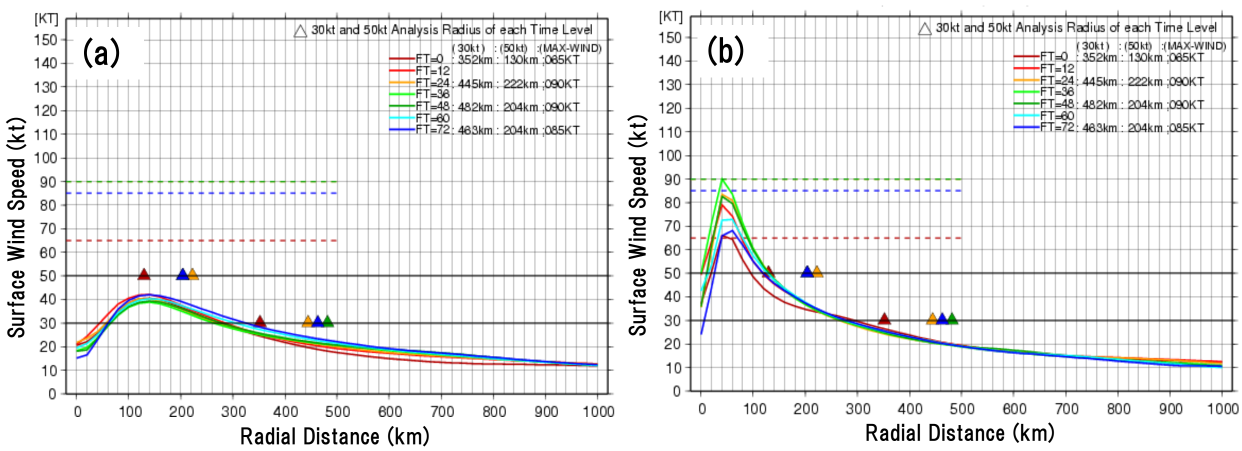

Figure 12: Time evolution of surface wind speed (kt) simulated by (a) 60km GSM and (b) 20km GSM for the typhoon Songda (see Figure 6 and Figure 7) in its development stage at the initial time of 12 UTC 30 August 2004. The surface wind speed for each forecast is shown in solid colored lines. The colored triangles represent the radius of 30kt and 50kt wind speeds analyzed in operation for each valid time. The colored broken lines represent the maximum sustained wind speed analyzed in operation for each valid time.

6. REFERENCES

JMA, 2007: Outline of the Operational Numerical Weather Prediction at the Japan Meteorological Agency (March 2007). Available at JMA Web site: *http://www.jma.go.jp/jma/jma-eng/jma-center/nwp/nwp-top.htm*

Kawai, H. and T. Inoue, 2006: A Simple Parameterization Scheme for Subtropical Marine Stratocumulus. *SOLA*, **2**, 017-020.

Komori, T., M. Yamaguchi, R. Sakai and Y. Takeuchi, 2007: WGNE Intercomparison of Tropical Cyclone Forecasts with Operational Global Models: Quindecennial Report, *WCRP Newsletter*, accepted. Available at WCRP Web site: *http://wcrp.wmo.int/Newsletter_index.html*

Murakami, H., T. Matsumura, R. Sakai, A. Noda, and S. Kusunoki, 2007: Verification of typhoon forecasts for a 20km-mesh high-resolution global model. *J. Meteor. Soc. Japan*, submitted.

Nakagawa, M., 2005: Precipitation forecasts by a high resolution global model at JMA. 'Hydrometeorological Applications of Weather and Climate Modelling': Extended abstracts of presentations at the seventeenth annual BMRC Modelling Workshop, 3-6 October 2005 (edited by Hollis, A. J.). *BMRC Research Report No.111*, 127-130.

Oowada, H., 2006: Simulated satellite image. *Meteorological Research Note*, **212**, 105-120. (in Japanese)

Smith, R. N. B., 1990: A scheme for predicting layer clouds and their water content in a general circulation model. *Quart. J. Roy. Meteor. Soc.,* **116,** 435-460.

Xie, S. C., and M. H. Zhang, 2000: Impact of the convection triggering function on single-column model simulations. *J. Geophys. Res.*, **105**, 14983-14996.